Solution and solid-state NMR structural investigations of the antimicrobial designer peptide GL13K in membranes

Nicole Harmouche[1], Christopher Aisenbrey[1], Fernando Porcelli[2], Youlin Xia[3], Sarah E. D. Nelson[3], Xi Chen[4], Jesus Raya[1], Louic Vermeer[1], Conrado Aparicio[4], Gianluigi Veglia[3], Sven-Ulrik Gorr[5], and Burkhard Bechinger[1*]

[1]Université de Strasbourg / CNRS, UMR7177, Institut de Chimie, 1, rue Blaise Pascal, 67070 Strasbourg, France

[2]DIBAF - University of Tuscia – Viterbo, Largo dell'Universita', Blocco D, 01100 Viterbo, Italy

[3]Department of Biochemistry, Molecular Biology & Biophysics, University of Minnesota, 321 Church Street SE, Minneapolis, MN 55455, USA

[4]Minnesota Dental Research Center for Biomaterials and Biomechanics and Department of Restorative Sciences, University of Minnesota School of Dentistry, 515 Delaware Street SE, Minneapolis MN 55455

[5]Department of Diagnostic and Biological Sciences, University of Minnesota School of Dentistry, 515 Delaware Street SE, Minneapolis MN 55455

*corresponding author: Burkhard Bechinger
4, rue Blaise Pascal, 67070 Strasbourg, France
Tel.: +33 3 68 85 13 03, FAX: +33 3 68 85 17 35, bechinge@unistra.fr

Key words: NMR structure, micelles, oriented bilayer, solid-state NMR, beta sheet membrane topology

Running title: GL13K membrane structure

ABSTRACT

The antimicrobial peptide GL13K encompasses 13 amino acid residues and has been designed and optimized from the salivary host-defense protein BPIFA2 to exhibit potent bacteriocidal and anti-biofilm activity against Gram-negative and Gram-positive bacteria as well as anti-lipopolysaccharide activity *in vitro* and *in vivo*. Here the peptide was analyzed in a variety of membrane environments by CD spectroscopy and by high resolution multidimensional solution NMR spectroscopy. Whereas in the absence of membranes a random coil conformation predominates, the peptide adopts a helical structure from residues 5 to 11 in the presence of DPC micelles. In contrast, a predominantly β-sheet structure was observed in the presence of lipid bilayers carrying negatively charged phospholipids. Whereas ^{15}N solid-state NMR spectra are indicative of a partial alignment of the peptide ^{15}N-^{1}H vector along the membrane surface, ^{2}H and ^{31}P solid-state NMR are indicative that in this configuration the peptide exhibits pronounced disordering activities on the phospholipid membrane which possibly relates to antimicrobial action. GL13K thus undergoes a number of conformational transitions including a random coil state in solution, a helical structure when diluted at the surface of zwitterionic membranes, and β-sheet conformations when occurring at high peptide-to-lipid ratio.

Abbreviations used

CD	circular dichroism
DHPC	1, 2- dihexanoyl-*sn*-glycero-3-phosphocholine
DMPC	1, 2-dimyrestoyl-*sn*-glycero-3-phosphocholine
DMPG	1, 2-dimyrestoyl-*sn*-glycero-3-(1'-rac-glycerol) sodium salt
DOPC	1, 2-dioleoyl-*sn*-glycero-3-phosphocholine
DOPG	1, 2-dioleoyl-*sn*-glycero-3-(1'-rac-glycerol) sodium salt
DPC	dodecylphosphosphocholine
HPLC	high performance liquid chromatorgraphy
LWHH	linewidth at half-height
MAS	magic angle spinning
NMR	nuclear magnetic resonance
NOE	nuclear Overhauser effect
NOESY	nuclear Overhauser effect spectroscopy
MALDI	matrix-assisted laser desorption ionisation
POPC	1-palmitoyl-2-oleoyl-*sn*-glycero-3-phosphocholine
POPE	1-palmitoyl-2-oleoyl-*sn*-glycero-3-phosphoethanolamine
POPG	1-palmitoyl-2-oleoyl-*sn*-glycero-3-(1'-rac-glycerol) sodium salt
POPS	1-palmitoyl-2-oleoyl-*sn*-glycero-3-phosphoserine
r.h.	relative humidity
SDS	sodium dodecyl phosphate
TFA	trifluoro acetic acid
TOCSY	total correlation spectroscopy

INTRODUCTION

Antimicrobial peptides and proteins (AMPs) are found in vertebrates, invertebrates, plants and bacteria, and several of these naturally occurring AMPs have inspired the design of novel AMPs [1, 2]. Synthetic peptide design aims to optimize strong antibacterial activity while avoiding bacterial resistance or mammalian toxicity. AMP sequences are highly diverse but certain principles for their design have emerged. Thus, short AMPs appear to require a balance of charged (R, K) with hydrophobic amino acids (I,V,F,Y,W) [3]. We have designed the peptide GL13K by analysis of the salivary protein BPIFA2 (BPI-fold family A member 2; previous names: Parotid Secretory Protein, PSP, SPLUNC2, C20orf70), a potential host-defense protein. The predicted structure of BPIFA2 was compared with the known structures of related BPI proteins [4] and the location of AMPs within the sequences of these proteins [5]. An initial peptide, GL13NH2 ($BPIFA2_{141-153}$), caused bacterial agglutination but did not exhibit bactericidal activity [6]. The distribution of cationic and hydrophobic residues was rebalanced by substituting charged residues with Lys residues, resulting in the peptide GL13K, which is bactericidal to Gram negative and Gram positive bacteria and their biofilms [6, 7]. Both GL13NH2 and GL13K also exhibit anti-lipopolysaccharide activity *in vitro* and *in vivo* [6].

Initial membrane interaction studies have shown that GL13K is highly selective for anionic bacterial model membranes (DOPG) compared to zwitterionic (neutral) eukaryotic model membranes (DOPC). In the presence of DOPC, the peptide exhibits a random coil conformation in circular dichroism (CD) spectroscopic investigations while it adopts a ß-sheet structure in the presence of DOPG [8]. Thus, as with other cationic amphipathic peptides, association to overall neutral membranes is probably too low to be detected by optical spectroscopies, which, due to light scattering, is limited to dilute solutions of small vesicles.

Here we use multidimensional solution NMR spectroscopy to investigate the high-resolution structure of GL13K in the presence of dodecylphosphocholine (DPC) micelles thereby representing its structure when associated with zwitterionic membranes at low P/L ratios (on average less than 1 peptide is associated with each micelle). Furthermore, a bacterial membrane was mimicked by POPE/POPG 3/1 mole/mole model bilayers. Its secondary structure preferences at this intermediate membrane lipid composition with only 25 mole% of negatively charged lipids was first determined by CD spectroscopy. Thereafter the peptide topology and its interactions with lipids were investigated by reconstituting GL13K labeled with ^{2}H and ^{15}N at specific sites into bilayers aligned along planar glass plates or in bicelles

that spontaneously align in the magnetic field of the NMR spectrometer, and measurement of the corresponding solid-state NMR spectra. Finally, the effect of the peptide on membrane packing was investigated by ^{2}H solid-state NMR of fatty acyl chain deuterated lipids. In this manner, a more comprehensive view of the GL13K interactions with membranes is obtained covering low and high peptide-to-lipid ratios as they occur with overall neutral, zwitterionic and negatively charged bacterial membranes, respectively.

MATERIALS AND METHODS

Materials

Amino-acid derivatives and other reagents for peptide synthesis were from Novabiochem-Merck (Darmstadt, Germany). All lipids were purchased from Avanti Polar Lipids (Alabaster, AL, USA). Water (HPLC grade), deuterium depleted water were from Sigma (St. Quentin Fallavier, France). Deuterated dodecylphosphocholine was purchased from Cambridge Isotope Laboratory, Andover, MA.

Peptide synthesis

The GL13K peptide with the sequence GKIIK**L**K**A**SLKLL-NH_2 was obtained by solid-phase peptide synthesis using a Millipore 9050 automated peptide synthesizer, the Fmoc (9-fluorenylmethyloxycarbonyl) chemistry and purified by semi-preparative HPLC as described previously for other antimicrobial peptides [9]. The underlined leucine-6 and the doubly-underlined alanine-8 positions were labeled with ^{15}N and $^{2}H_3$, respectively, by incorporating the isotopically labeled fmoc-precursors (Euriso-top, Paris, France or Isotec® Sigma-Aldrich, St Quentin Fallavier, France). The identity and high purity of the product (>90%) was confirmed by HPLC, MALDI mass spectrometry and NMR spectroscopy. After lyophilisation, the TFA counter ions were exchanged in 5% acetate (v/v). The randomized peptide GL13K-R1 with the sequence IGIKLLKSKLKAL-NH_2 was obtained from AAPPTec. (Louisville, KY, U.S.A.)

Micellar Sample Preparation and Solution NMR Spectroscopy

The lyophilized peptide was dissolved to a final concentration of 1.9 mM in aqueous solution (10% D_2O, 90% H_2O) containing 186 mM of perdeuterated DPC (Cambridge Isotope Laboratories; Andover, MA) and 10 mM of phosphate buffer at pH 5. All the NMR

experiments were carried out at 298 K on a Bruker 700 MHz spectrometer (Bruker Biospin, Billerica, MA). The homonuclear 2D TOCSY [10] spectrum (70 ms) and 2D NOESY [11] (100 -250 ms mixing time) experiments were acquired in the phase-sensitive mode using time proportional phase incrementation. A WATERGATE pulse sequence [12] was used for solvent suppression. During the isotropic mixing time, a DIPSI-2 pulse sequence [13] was used in the TOCSY experiments. In all experiments the spectral width was 8000 Hz in both dimensions. 2D data were zero filled to 4096 points in the direct and to 1024 points in the indirect dimension and then processed using a sine-bell squared window function shifted between 60°and 90° before Fourier transformation. For baseline correction, a 6th order polynomial function was used.

All the spectra were processed using NMRPipe [14] and the data were analyzed using Sparky [15]. The traditional resonance assignment approach described by Wüthrich [16] was applied.

Structure Calculation.

A total of 151 NOEs, including 70 intra- and 81 inter-residue NOEs, were used for structure calculation. NOE cross-peaks from 100 - 250 ms mixing time [^{1}H-^{1}H] NOESY spectra were integrated and classified as strong, medium and weak corresponding to distance restraints of 1.8-2.9, 1.8-3.6 and 1.8-6.0 Å, respectively. The GL13K structural ensemble was calculated starting from the extended structure and minimized using a hybrid simulating annealing (SA) protocol present in XPLOR-NIH [17]. 100 conformers were generated at an initial temperature of 1000 K with 50000 high temperature steps and 6000 cooling steps. Structural refinement was carried out by introducing Lennard-Jones potentials and van der Waals and electrostatic interactions using an initial temperature T_i of 1000K with 10000 cooling steps with 5 fs step size. The final refinement of the structural ensemble was calculated at T_i of 600 K with 50000 cooling steps with 1 fs step size.

Circular dichroism spectroscopy

Lipids POPE:POPG (3:1mol:mol) and POPC:POPS (3:1 mol:mol) were mixed in chloroform, dried under a stream of nitrogen gas and kept under vacuum overnight, after which they were rehydrated with 5 or 10 mM Tris HCl at pH 7.4 and subjected to 3 freeze/thaw cycles. Small unilamelar vesicles (SUVs) were obtained after less than 1 min of tip sonication with a Bandelin Sonopuls HD 200 (Berlin, Germany). Circular

dichroism (CD) spectra were recorded from 250 to 190 nm (spectral resolution: 1 nm, data pitch: 1 nm, scanning speed: 50 nm/min) using a Jasco J-810 or a J-815 spectropolarimeter (Jasco, Tokyo, Japan) and quartz cell with 1.0 mm path length.

For lipid titration experiments the samples containing 60 μM of GL13K peptide in 5 mM Tris-HCl buffer pH 7.4 were maintained at 37 °C for titration with POPE:POPG SUVs and at 25°C for the one with POPC:POPS. A stock solution of SUVs at 13.6 mM was used for the peptide solution titration at different peptide to lipid ratios. A total of 9 spectra were acquired and averaged for each condition. A mock titration of lipids into 5 mM Tris HCl without peptide was used to generate control curves, which were subtracted from the CD-spectra of peptide-containing samples. The resulting intensities in millidegrees were converted to mean residue molar ellipticity (MRE=$\theta/10nCl$, where n is the number of peptide bonds, C the concentration in M, and l the path length in cm).

For obtaining the pH-dependent circular dichroism (CD) spectra of GL13K and GL13K-R1 the peptides were dissolved at 0.1 mM concentration in a series of sodium borate buffers at pH 8.5; 9; 9.2; 9.4; 9.6; 9.8; 10; 10.2; 10.4; 10.6. CD spectra were acquired with solvent subtraction. To examine the percentage of secondary structure of peptides, the spectra were fitted using three different programs (CDSSTR, CONTINLL and SELCON3) in CD Pro [18] and the averaged percentage is reported. Alternatively, a home-made programme was used fitting the experimental spectra by finding optimal linear combinations of published peptide spectra.

Sample Preparation for mechanically oriented membranes

A homogeneous mixture of POPE:POPG (3:1/m:m) and [^{15}N-L6, $^{2}H_3$-A8]-GL13K was obtained by co-dissolving the components in chloroform/methanol (1:1/v:v). The solution was spread onto ultra-thin cover glasses (8x22 mm, Marienfeld, Lauda-Konigshofen, Germany) and dried, first in air and thereafter in high vacuum overnight. Membranes were equilibrated at 93 % relative humidity, and where it was necessary to obtain hydration in the liquid-disordered state, the membranes were further exposed to higher temperatures (310 K) before the glass slides were stacked on top of each other and sealed in Teflon then in a plastic wrapping.

Sample Preparation for magnetically aligned bicelles

2.5 mg of [^{15}N-L6, $^{2}H_3$-A8]-GL13K was added to a solution of 131 mM 1,2-dihexanoyl-*sn*-glycero-3-phosphocoline (DHPC). Then this solution was added to the long chain lipids

DMPC (1.2-dimyristoyl-*sn*-glycero-3-phosphocoline and DMPG (1,2-dimyristoyl-*sn*-glycero-3-phospho-(1'-rac-glycerol); DMPC:DMPG 4:1 mole/mole). The lipid composition was arranged so that the DMPC:DMPG/DHPC sample has a lipid concentration of 28% (w:v) and a molar ratio q = [DMPC:DMPG]/[DHPC] = 3.5. To mimic physiological conditions a suitable volume of 100 mM NaCl in water at pH = 7.4 was added thus the sample contained 78 wt% water for all preparations (h = mass of water over the total mass of the system (phospholipids and water)). Hydrated samples were precipitated in a 5804R Eppendorf benchtop centrifuge with a model F-45-30-11 rotor (Eppendorf AG, Hamburg, Germany) at 6500 rpm (~4500 g) for 5 min and vigorously vortexed. The samples were then frozen in liquid nitrogen for 30 s, heated at 40°C for 10 min in a water bath, vigorously vortexed, and centrifuged again at 6500 rpm for 5 min at 4°C. This cycle was repeated three times until a homogeneous suspension (viscous and translucent) was obtained at room temperature.

Solid-state NMR spectroscopy

NMR experiments were carried out on Bruker Avance spectrometers operating either at 11.7 T (^{1}H frequency 500 MHz) or at 17.7 T (750 MHz).

^{31}P NMR spectra were acquired at 202.4 MHz (11.7 T) using a phase-cycled Hahn-echo pulse sequence with gated broadband proton decoupling [19]. Typical acquisition parameters were as follows: spectral window, π/2 pulse width and recycle delay of 100 kHz, 6 μs and 5 s, respectively, for mechanically aligned samples and of 20 kHz, 7.1 μs and 5 s, respectively, for aligned bicelles. Typically, 1024 scans were recorded. A line broadening of 50 Hz was usually applied prior to Fourier transformation. Quadrature detection was used in all cases. Phosphorus chemical shifts were calibrated relative to H_3PO_4 (85% in H_2O, 0 ppm). Samples were allowed to equilibrate for at least 20 min at (40 ± 1)°C before the NMR signal was acquired.

^{2}H NMR spectra were acquired at 76.8 MHz by means of a quadrupolar echo pulse sequence [20], with a π/2 pulse width of 7.5 μs and a 50 μs interpulse delay for mechanically oriented samples (for bicelles 4.5 μs, and 100 μs, respectively) and a recycle delay of 1 s. Typically, 20000 scans were recorded and a Lorentzian noise filtering width of 200 Hz was applied prior to Fourier transformation from the top of the echo signal. Quadrature detection was used in all cases. The reference for solid-state deuterium powder patterns was set to zero and the position of the carrier placed in the middle of the symmetric Pake pattern (powder spectrum). Samples were allowed to equilibrate for at least 20 min at

(40 ± 1) °C before the NMR signal was acquired. The S_{CD} order parameters in bilayer membranes are proportional to the quadrupolar splittings [21, 22]: $S_{CD}=4\Delta\nu_Q/3\,A_Q$, where A_Q is 167 KHz.

Proton-decoupled ^{15}N cross polarization (CP) spectra were acquired at 50.7 MHz (11.7 T) for mechanically aligned samples and at 76.8 MHz (17.7 T) for bicelles. A CP pulse sequence was used, with a spectral width, acquisition time, CP contact time, π/2 pulse width, and recycle delay of 50 kHz, 10 ms, 0.8 ms, 10 μs and 3 s, respectively, for mechanically oriented samples and of 50 kHz, 10 ms, 0.4 ms, 8 μs and 2 s for magnetically oriented bicelles. 67000 and 100 000 scans were accumulated for mechanically oriented samples and bicelles, respectively. The spectra were recorded at temperatures above the gel to liquid phase transition. A 200 Hz exponential line broadening was applied before Fourier transformation

Spectral simulations

All spectra were simulated using the Mathematica 3.0 (Wolfram Research, Champaign, IL, USA). The CSA tensors were expressed in spherical coordinates and spectra were calculated by integration of all possible orientations using the assumed orientational distribution as weighting factor and folded with an inherent line broadening of 300 Hz. For the ^{15}N backbone the CSA tensor σ_{11}=62.5, σ_{22}=77.3 and σ_{33}=233.5 was taken into account [23], where σ_{11} and σ_{33} are in the plane of the peptide bond defined by the NH vector and the $C_{carboxyl}N$ vector. The angle between the $C_{carboxyl}N$ vector and σ_{33} is 105°. For ^{31}P an axial-symmetric in which the tensor elements were adjusted for the best fit was considered. The line broadening was 1600 Hz to simulate the ^{31}P solid-state NMR spectra and 2kHz for the ^{2}H solid-state NMR spectra.

RESULTS

Solution NMR studies in DPC micelles.

The high-resolution structure of the GLK13 peptide was determined in the presence of DPC micelles by multidimensional solution NMR spectroscopy. A combination of 2D [^{1}H-^{1}H] TOCSY and 2D [^{1}H-^{1}H] NOESY spectra was used to assign specific resonances and to get NOE connectivities. Because of the line broadening, due to the slow tumbling of peptide in micelles, the J coupling constants could not be extracted [24, 25]. Table S1 reports the resonance assignment with the exception of alanine 8 which carried a deuterated side chain. Amino acid spin systems were assigned following the sequence-specific method (NOESY-walk) reported by Wüthrich [16] and a total of 151 NOEs (81 inter-residue and 70 intra-residue) were identified. Several $d_{NN}(i, i+1)$, $d_{\alpha N}(i, i+1)$ and $d_{\alpha N}(i, i+2)$ were identified along the backbone of peptide. Figure 1 A and B show the backbone NOE pattern and the chemical shift index (CSI), respectively, for the peptide in DPC micelles. The concomitant presence of both a deviation of more than -0.1 ppm of the CSI value and the existence of $d_{\alpha N}$ (i,i+3) and $d_{\alpha N}$ (i,i+4) connectivities [26], are indicative of the presence of α-helical structures. The structures obtained from simulated annealing calculations using XPLOR-NIH confirmed this first analysis. Figure 2A and B show the superposition of the 20 lowest energy conformers. The reported ensemble shows an α-helical structure between Lys-5 and Lys-11 (Figure 2C) and the superposition of backbone atoms in this region gives a RMSD of 0.29 ± 0.13 Å for backbone and a RMSD of 1.36 ± 0.40 Å for the heavy atom side chains. In Fig. 2D the RMSD versus residue, blue for side chains and red for backbone, is reported.

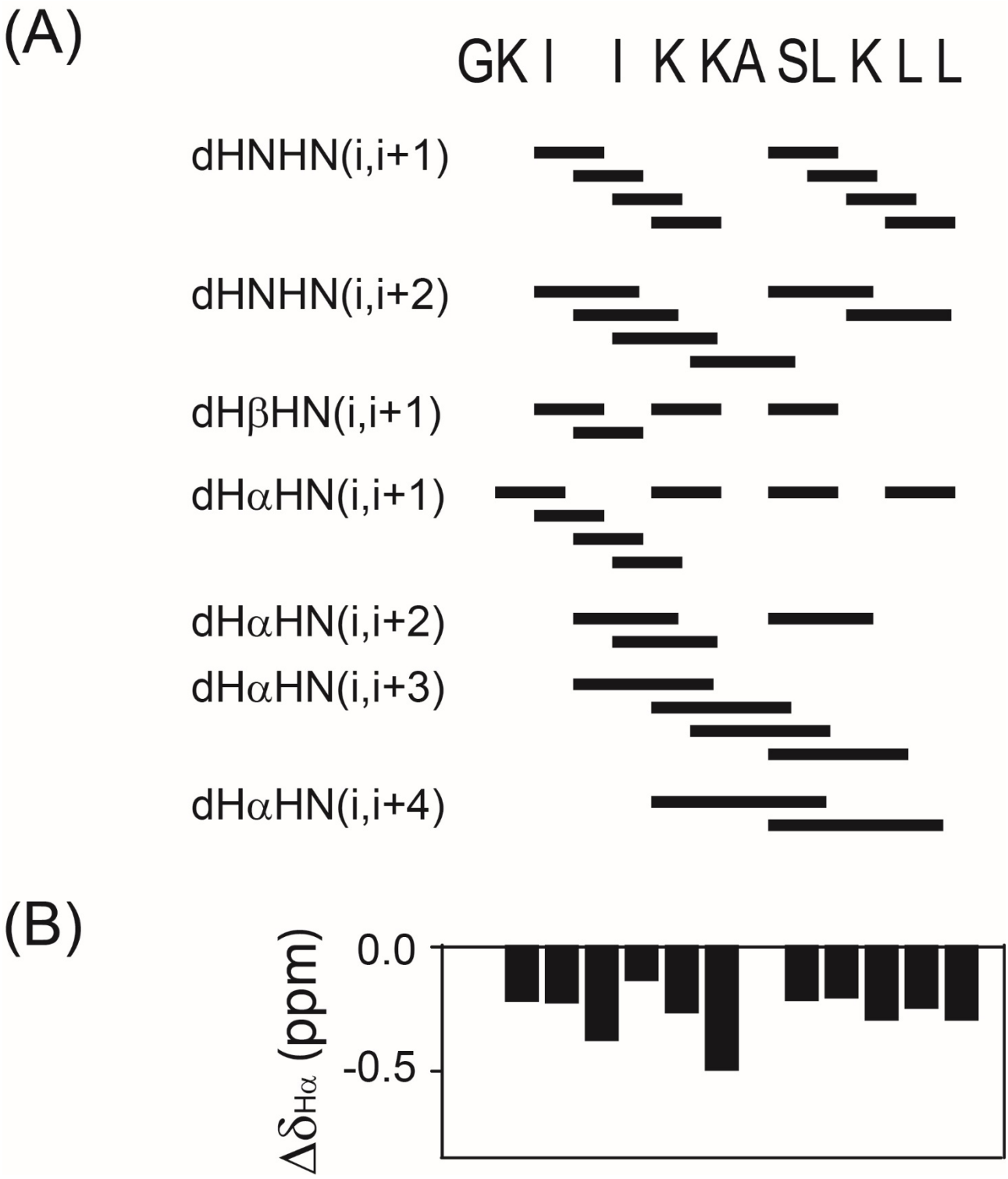

Figure 1: (A). Graphical summary of NOE constraints obtained from 1.9 mM GL13K in the presence of 189 mM DPC in 10 mM phosphate buffer (pH 5) at 298 K. (**B).** ^{1}H chemical shift index of $C_{\alpha}H$ for GL13K. Negative values are indicative of helical conformations [26].

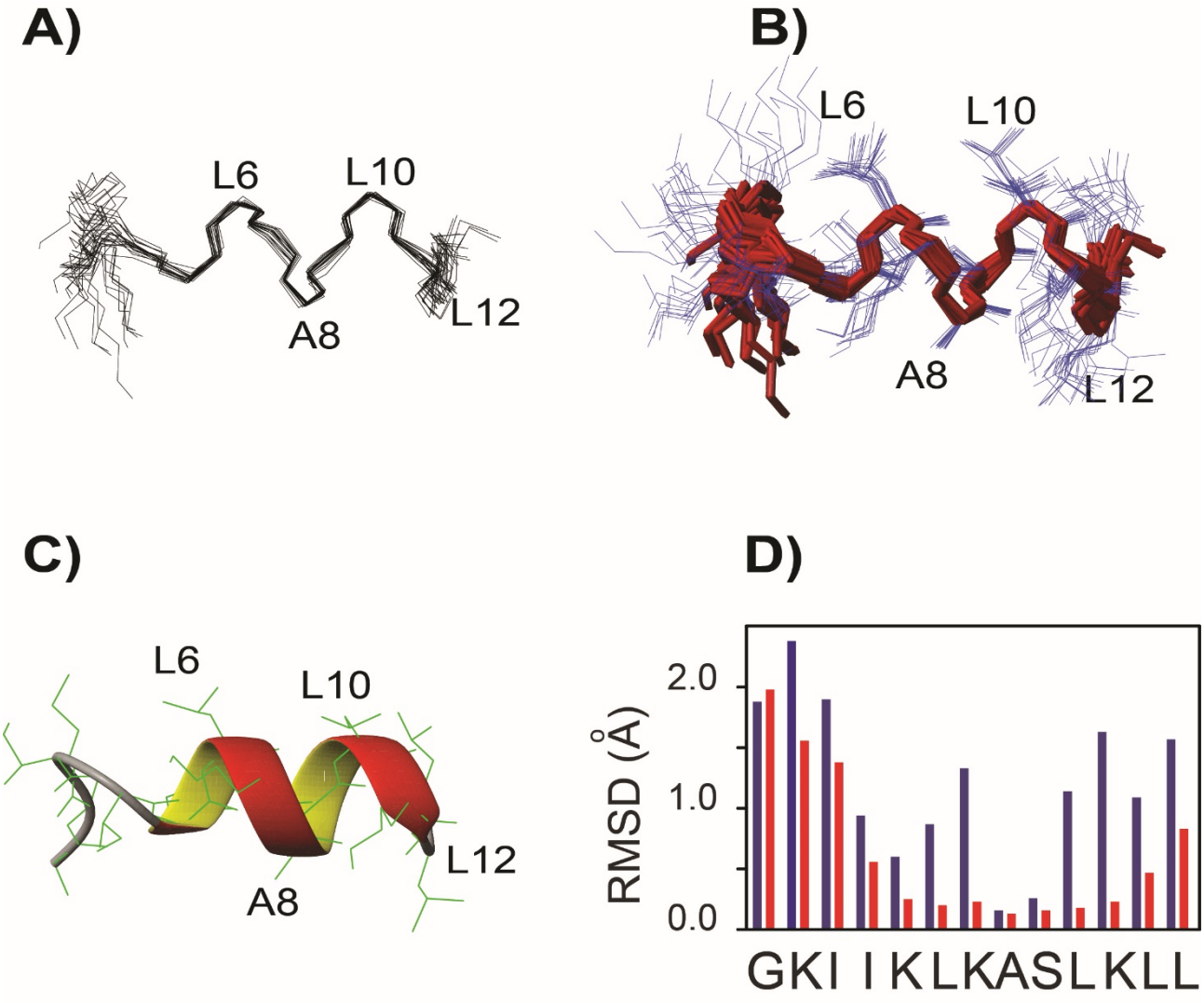

Figure 2: NMR structural ensemble of GL13K in DPC micellar environments using NOE restraints represented in Fig. 1. A. Twenty lowest energy conformers showing the convergence for the backbone and side chains (B.). C. Representative average structure of GL13K. D. Residue-dependent root mean-square deviations (RMSD) for backbone (red) and side-chains (blue) comparing the twenty lowest energy conformers. The structures were fit onto the average conformation. and residues 5-11 were used for the superposition of the conformers.

CD spectroscopic titrations

The experimental conditions used during the above NMR structural analysis are characterized by a high DPC-to-peptide molar ratio, with on average less than one peptide per micelle. The helical structure thereby represents the peptides in their isolated, monomeric state as they occur at low peptide association with e.g. zwitterionic membranes. Indeed, the helical secondary structure requires high detergent concentrations (Figure S1) and previous CD experiments are indicative that the peptide

only weakly interacts with zwitterionic membranes [8]. Furthermore, these experiments showed, that GL13K adopts β-sheet conformations when associated with DOPG bilayers. In order to extend these previous investigations, CD spectra were also recorded in the presence of vesicles encompassing an intermediate amount of negatively charged lipids characteristic of bacterial membranes, namely POPE:POPG 3:1, as well as POPC:POPS 3:1 mole/mole small unilamellar vesicles (Figures 3A,B). As in previous investigations, considerable scattering hampers the evaluation of spectra < 200 nm and deconvolution into different secondary structures [8]. However, the spectra closely resemble those obtained in the presence of DOPG membranes where the negative intensities at 217 nm where taken as an indicator of β-sheet conformations [8]. Therefore, the transition from random coil in solution to β-sheet-rich conformations already occurs with liposomes containing moderate concentrations of negatively charged lipids. Interestingly, the transition occurs in a step-wise manner once the concentration of POPE/POPG exceeds 600 μM (Fig. 3A).

The calculated net charge of GL13K is +5 at pH=7 and 0 at pH=14 (pI). To further investigate the effect of peptide charge on the structural preferences of GL13K a pH titration was performed by CD spectroscopy, using the pH range with the highest change in net charge. A quantitative analysis of the spectra at neutral pH is indicative of 10-15% α-helix, 25-30% β-sheet/β-turn and 55 % unordered (Fig. 3A-C). When increasing the pH up to 10.6 about 20% of the random coil converts into additional β-sheet contributions in a pH-dependent manner (Fig. 3C). The isosbestic point at 210 nm is indicative of a two-state equilibrium. Notably, this transition was absent for the randomized sequence GL13K-R1 (IGIKLLKSKLKAL-NH_2, cf. [6]; Fig. 3D). In contrast the latter peptide shows a higher helix content at high pH.

Solid-state NMR studies of GL13K associated with POPE/POPG bilayers.

In a next step the GL13K peptide labeled with ^{15}N at leucine-6 and with methyl-deuterated alanine at position 8 was reconstituted into oriented phospholipid bilayers with a phospholipid composition mimicking bacterial membranes, and investigated by solid-state NMR spectroscopy [27]. The NMR parameters observed in such samples are dependent on the molecular alignment relative to the magnetic field direction of the NMR spectrometer (B_o). When the sample normal is oriented parallel to B_o the ^{15}N chemical shift and ^{2}H quadrupolar splittings can be analyzed in terms of peptide topology and

orientational distribution [27]. Furthermore the effects of the peptide on the orientational order, packing and macroscopic phases can be investigated using ^{31}P solid-state NMR [28].

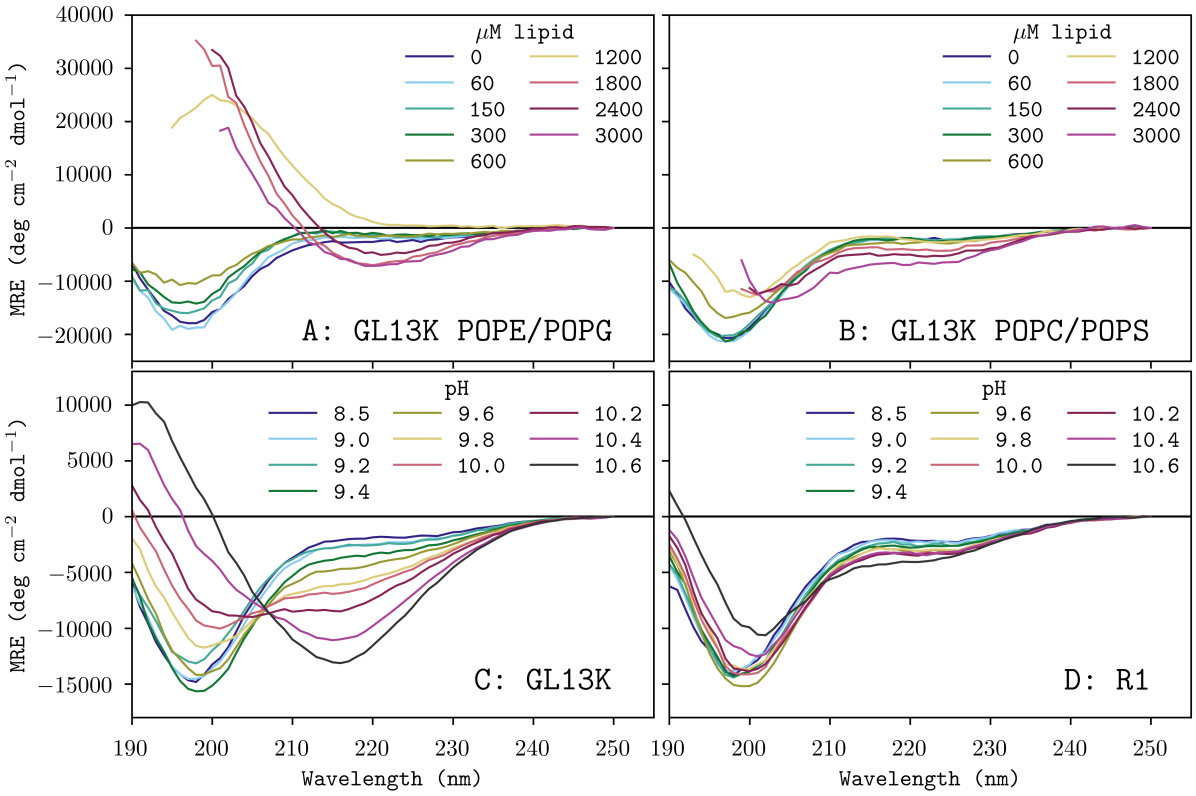

Figure 3. (A) CD spectral titration of 60 μM GL13K with 0 to 3000μM of POPE:POPG (3:1 mole/mole) SUVs at 37°C in 10 mM Tris HCl, pH 7.4 and (B) of POPC:POPS SUVs (3:1 mole/mole) at 25°C in 5 mM Tris HCl, pH 7.4. Spectra are corrected with control curves of SUVs only but peptide-induced liposome aggregation causes some of the spectra to be severely affected by light scattering. Therefore, spectra at the highest lipid concentrations were truncated < 200 nm. CD spectra of GL13K (C) and GL13K-R1 (D) in buffers from pH 8.5 to 10.6. GL13K but not GK13K-R1 gradually shifts from random coil to more β-turn secondary structure with increasing pH. GL13K-R1 but not GL13K exhibits more α-helix at high pH.

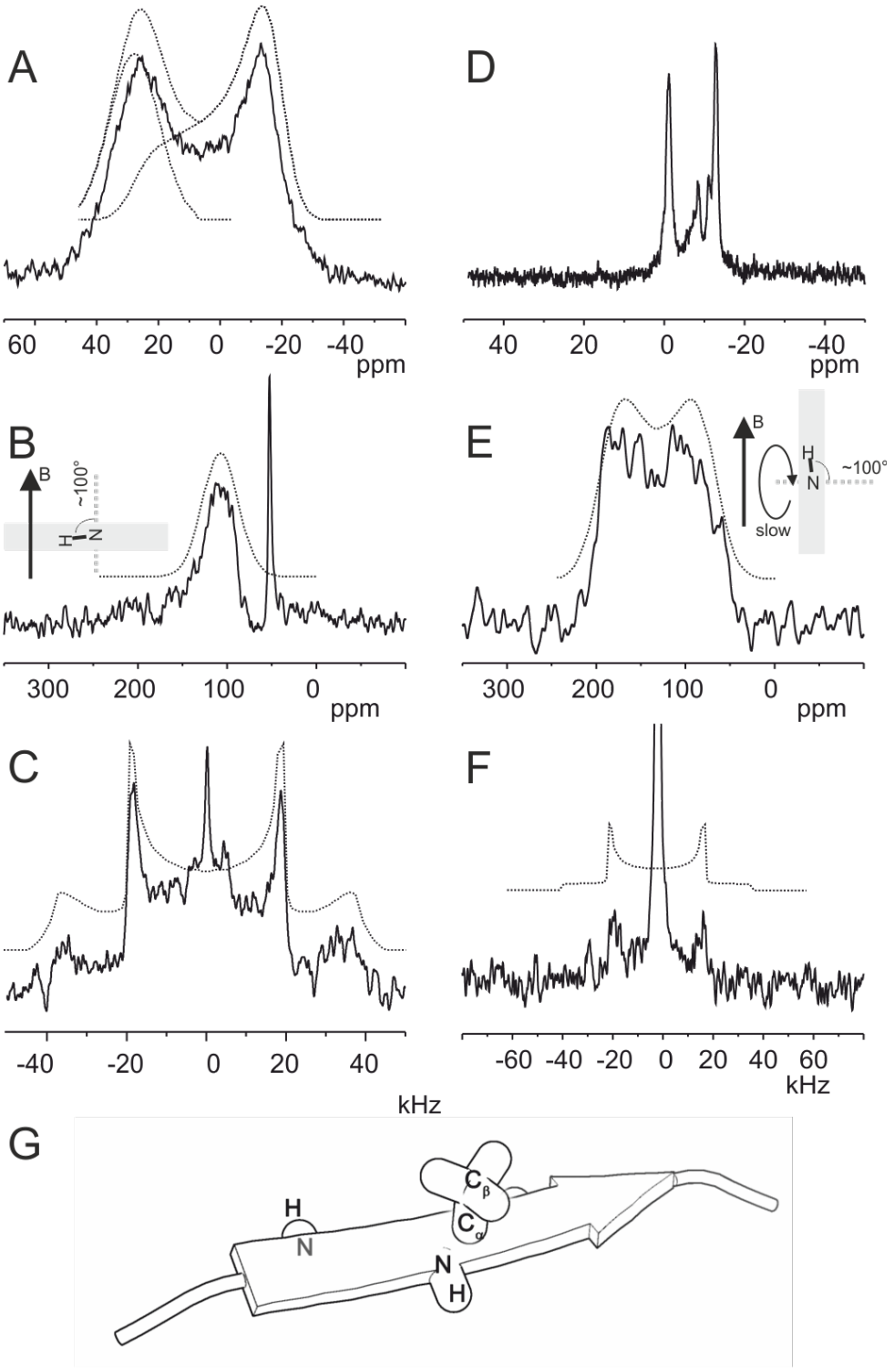

Figure 4: Solid-state NMR spectra of [^{15}N-Leu6, ^{2}H-Ala8]-GL13K reconstituted into mechanically oriented POPE:POPG (3:1) bilayers (A-C) and into [DMPC:DMPG]/[DCPC] magnetically aligned bicelles (D-F) at 310K. The first row (A, D) shows the corresponding ^{1}H-decoupled ^{31}P solid–state NMR spectra of the sample phospholipids, the second row (B, E) the ^{15}N NMR spectra and the third row (C, F) the ^{2}H-NMR spectra obtained from the reconstituted [^{15}N-Leu6, ^{2}H-Ala8]-GL13K peptide. The ^{31}P solid-state NMR and the mechanically oriented samples were investigated at 11.8 T, the ^{15}N and ^{2}H spectra of the peptide in bicelles at 17.7 T (E, F). The dotted traces correspond to simulated spectra: A:

36% oriented with 18.8 ppm LWHH and 64% powder with 11.8 ppm LWHH, B: Oriented with an angle between the NH bond and the membrane normal of 100° (membrane normal parallel to magnetic field) and 47 ppm LWHH C. powder pattern line shape (2/3) combined with a spectrum that results from a mean alignment of the Cα-Cβ bond parallel to the membrane normal with 45° mosaicity (1/3). E: integral of all possible orientations with an angle between NH and membrane normal of 100° (membrane normal perpendicular to magnetic field) and 47 ppm LWHH. F. Powder pattern line shape. The membrane alignment is sketched as a grey bar next to panels B and E together with the approximate alignment of the N-H bond. A sheet with the relative orientations of the NH bond and the Cα-Cβ vector of the alanine side chain in shown in panel G.

Figure 4A shows the ^{31}P solid-state NMR spectrum of POPE/POPG 3/1 mole/mole bilayers in the presence of 2 mole% GL13K supported by glass plates that are oriented with the sample normal parallel to the magnetic field direction of the spectrometer (B_o). The intensities around 30 ppm are indicative of phospholipids that are oriented with their long axis parallel to B_o [28]. However, when compared to pure lipid bilayers (cf. Fig. 3 in [28]) the line width of this 'oriented' signal intensity is quite broad (LWHH ~19ppm). Furthermore, a major fraction of resonances extends over the full chemical shift anisotropy, where intensities close to -15 ppm are indicative of phopholipids in a perpendicular orientation relative to the magnetic field direction (coinciding with the sample normal). Among other possibilities, the combination of 36% lipids oriented with their long axis parallel to the sample normal (18.8 ppm LWHH) and 64% randomly oriented (powder pattern) results in a related line shape. Regardless of what is the detailed supramolecular assembly the spectra are indicative that the peptide has a high capacity to disrupt the membrane orientational order. In comparison the disruption of orientational order at comparable P/L is much higher for GL13K than for other cationic amphipathic antimicrobial peptides such as the helical magainins [28-30], phyloseptins [31] or the β-sheet arenicin [32]. On the other hand dermadistinctin K [9] and protegrin [33] also show pronounced disordering effects when investigated in the context of supported lipid bilayers.

Furthermore, the ^{15}N and ^{2}H solid-state NMR spectra of the labeled peptide within the same sample were investigated (Fig. 4B, C). To first approximation the ^{15}N spectrum represents the alignment of ^{15}N-H vectors relative to the magnetic field direction and thus the main axis of helical peptides relative to the sample normal [34]. Whereas values around 200 ppm are associated with transmembrane helical peptides (or NH vectors parallel to the sample normal), chemical shifts < 100 pm are indicative of perpendicular orientations [34]. When reconstituted into mechanically supported phopholipid bilayers where the

sample normal is oriented parallel to the magnetic field direction most ^{15}N intensities appear at 85 ppm with a LWHH of ~47 ppm, indicating that the N-H vectors are oriented predominantly perpendicular to B_o (Fig. 4B). An angle between NH and B_o of about 100° represents well the spectral maximum.

Finally, the ^{2}H quadrupolar splitting of the $^{2}H_3C$ alanine methyl groups is a function of the C_α-C_β angle relative to the magnetic field direction/sample normal and can be very sensitive to even small changes in membrane alignment [35]. Similar to the ^{31}P solid-state NMR spectra the ^{15}N and ^{2}H spectra exhibit broad spectral line shapes that could arise from a combination of powder pattern line shapes, where the elevated shoulders at ±35 kHz could arise from circular orientational distribution, or represent a composite of oriented contributions and powder pattern line shapes (Fig. 4C). The latter contributions are expected to arise e.g. from a twisted β-sheet.

The GL13K peptide was also investigated in the presence of phospholipid bicelles which at a lipid concentration of 28% (w:v), a molar ratio q = [DMPC:DMPG]/[DCPC] of 3.5 and a temperature of 310K have been shown to align in the magnetic fields of NMR spectrometers [36, 37]. Interactions of the peptide with the anionic bilayer assure that the cationic GL13K also aligns in the magnetic field. In contrast to the mechanically oriented sample the bilayer normal of the bicelle is oriented perpendicular to B_o.

Due to fast rotation of the phospholipids around their long axis the ^{31}P NMR spectra are characterized by two components, namely the averaged tensor elements $\sigma_{\parallel}$ and $\sigma_{\perp}$, representing the component parallel and perpendicular to the rotation axis, respectively [38, 39]. Whereas in the mechanically oriented sample the interaction of the ^{31}P chemical shift is represented by $\sigma_{\parallel}$, tilting the membrane by 90° aligns $\sigma_{\perp}$ parallel to B_o and thereby represents the observed chemical shift. Therefore, in Figure 4D the signal intensities at -14 and -11 ppm are indicative of oriented PC and PG components, whereas the intensity at ~0 ppm has been associated with the short chain lipids DHPC that freely change orientation by diffusing fast within the bicellar rim structure [40, 41].

The ^{15}N spectrum exhibits a broad distribution of resonances ranging from 224 to 65 ppm, indicative of NH vector orientations ranging from parallel to perpendicular relative to B_o. Rotation around the bilayer normal, which in the bicellar case is oriented perpendicular to B_o, results in many different peptide orientations relative to B_o. Indeed, taking into account the 100° NH alignment relative to the sample normal that has been found to represent well the ^{15}N spectrum of the mechanically oriented samples (Fig. 4B),

also explains well the bicellar ^{15}N spectrum (Fig. 4E) under the condition that motional averaging around the bilayer normal is slow on the 10^4 Hz time scale of the ^{15}N chemical shift anisotropy [42]. Finally, the ^{2}H solid-state spectrum of GL13K associated with the bicellar system is shown in Figure 4F. The signal-to-noise remains modest despite three days of signal averaging and, therefore, the spectrum cannot be analyzed in detail. For comparison, a powder pattern line shape, making a major contribution also to Fig. 4C, is shown on top of the spectrum showing that the maximal peak intensities can be associated with such a (close to) random distribution of C_α-C_β vectors.

Finally, we used ^{2}H solid-state NMR spectroscopy to investigate the effect of GL13K on the fatty acyl chain packing of the bilayers. Mixed POPE/POPG membranes were studied where all ^{1}H positions of the palmitoyl chain of either POPE or POPG in the bacterial mimetic membrane were exchanged by deuterium. The resulting ^{2}H solid-state NMR spectra encompass signals from the different CD_2 and one CD_3 segment, each contributing a powder pattern line shape, where the distance between the two main peaks defines the quadrupolar splitting [21, 43]. Without motions the static splitting would amount to 125 kHz. However, in the liquid crystalline bilayers investigated here motions and cis-trans isomerisations result in a considerable reduction as evident from the ^{2}H solid-state NMR spectra shown in Figure 5A,C. Notably, the segments exhibit more motional freedom in the hydrophobic interior when compared to the region of the carbonyls. The order parameter profiles were extracted separately for both types of phospholipid (Fig. 5B,D). In the presence of 2 mole% GL13K a considerable decrease in the packing order is observed for both lipids. The decrease is about 20 % for the POPE and 10 % for POPG palmitoyl chains.

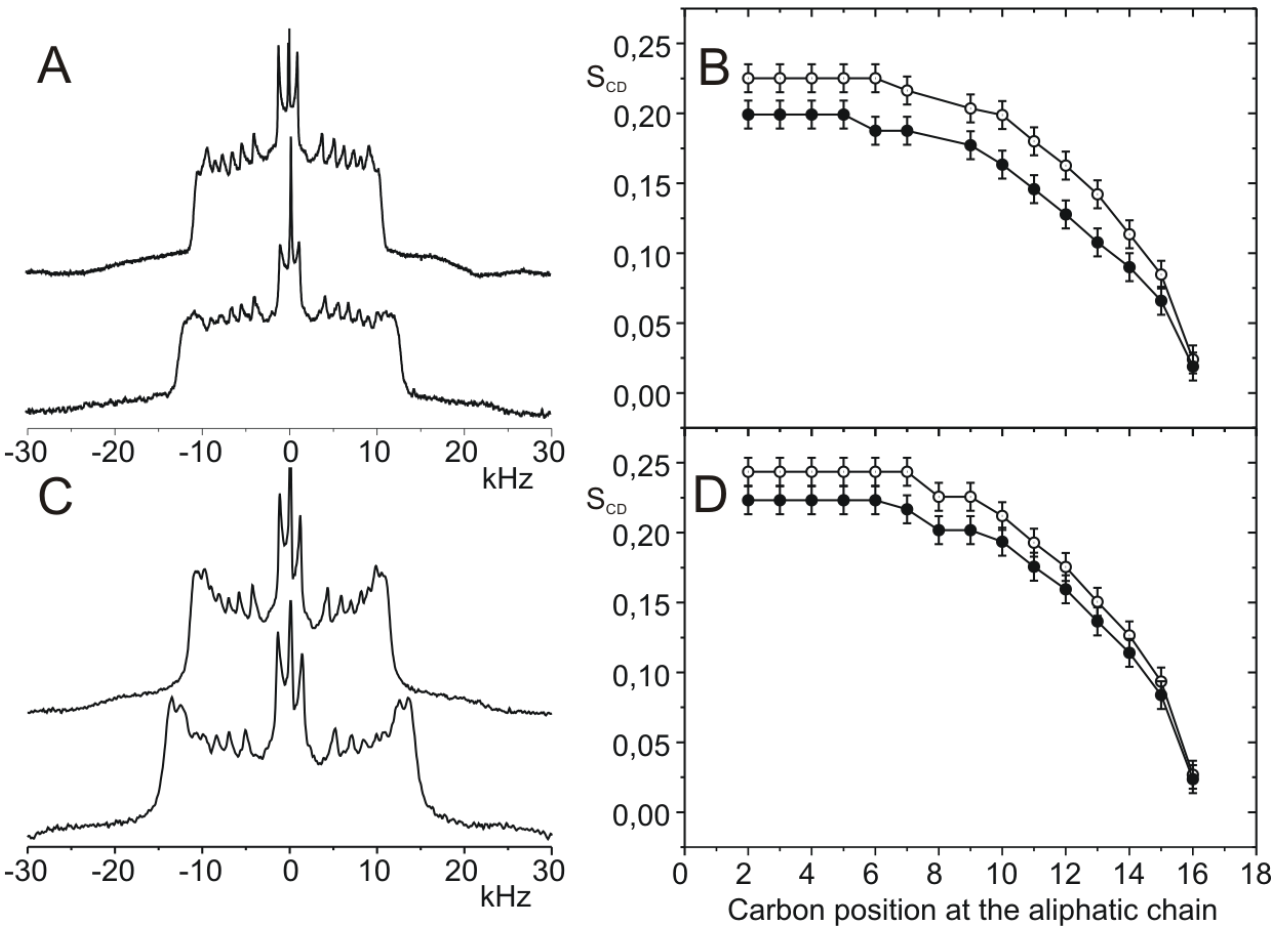

Figure 5: ^{2}H-NMR spectra of [^{15}N-L6, ^{2}H-A8]-GL13K embedded into POPE:$^{2}H_3$-POPE:POPG liposomes (A) and into POPE: POPG: $^{2}H_{31}$POPG (C), at 310K in 10mM Tris HCl buffer. In each panel, the spectra in the presence of 2 mol % GL13K are shown above the spectra obtained from pure lipid bilayers. (B and D) Corresponding order parameters as a function of the carbon position on the aliphatic chain in the presence (filled circles) and absence (open circles) of GL13K.

DISCUSSION

GL13K is a short cationic, amphipathic peptide that efficiently interacts with membranes. We have previously found that GL13K is effective against the Gram-negative bacterium *Escherichia coli* (MIC: 5 μg/ml), and *Pseudomonas aeruginosa* (MIC: 8μg/ml) [6], whereas the peptide is not effective against the oral Gram negative pathogen *Porphyromonas gingivalis* [6]. Similarly, activity is limited against Gram positive bacteria, including *Streptococcus gordonii* [MIC (minimum inhibitory concentration): 64μg/ml] (Hirt and Gorr, unpublished observations), *Staphyloccocus aureus* (MIC of 41μg/ml)(Gorr, unpublished observations) and *Enteroccocus faecalis* (MIC >512μg/ml) (Hirt and Gorr, unpublished observations). However, the peptide kills up to 99.99% of the bacteria in existing biofilms of *P. aeruginosa* [7].

Here we demonstrate that GL13K exhibits random coil conformations in aqueous solution, helical structures in DPC micelles and β-sheet-rich conformations in the presence of liposomes composed of 25% negatively charged lipids, which were also observed previously when associated with DOPG liposomes [8]. In the presence of phosphatidylcholine liposomes membrane association of this highly charged peptide is low and the CD spectra represent mostly the peptide that remains in solution. Because light scattering interferes with optical spectroscopies, in particular when extending into the UV spectral region, only dilute liposomal suspensions have been investigated by CD spectroscopy. In contrast, during the NMR structure analysis presented here high DPC concentrations were used, which brings the binding equilibrium to the membrane-associated state. Therefore, the NMR structural data in combination with previously published investigations [8] indicate that depending on the membrane composition and other environmental parameters, GL13K adopts helical or β-sheet-rich secondary structures in the presence of membranes.

The helical structure determined in the presence of DPC micelles (detergent/peptide molar ratio = 100) extends from residues 5 to 11. The resulting three-dimensional fold results in a small hydrophobic surface of leucines 6 and 10, opposed by lysines 5, 7 and 11 which suggest an interfacial association (Fig. 6). As with other cationic amphipathic peptides the resulting hydrophobic interactions alone are weak [44] but membrane association is enhanced by electrostatic attraction [8, 45] Notably, in the DPC micellar system, where one micelle is made of about 40 detergent molecules [46], there is on average less than one peptide per micelle which probably also represents the situation when the peptide associates with neutral membranes and the resulting low peptide-to-lipid ratios. Due to its weak interactions with zwitterionic membranes the NMR structure presented here is thereby the only biophysical data of the peptide describing the membrane-associated state at low concentrations.

In the presence of DOPG membranes CD spectroscopy has revealed a predominantly β-sheet conformation [8]. Clearly the high negative charge density of this lipid bilayer increases the local peptide concentration along the membrane surface and thereby the apparent binding constant. Here we extended these investigations to intermediate concentrations of negatively charged lipids by adding 75% of PE, a lipid preponderant in bacterial membranes. Also under these conditions CD spectra are indicative of a β-sheet conformation of GL13K (Fig. 3A,B). The combination of ^{15}N and ^{2}H

solid-state NMR data suggest a predominant alignment of the sheet along the membrane surface as depicted in Figure 4G, with considerable twist, and slow rotational diffusion around the membrane normal probably due to peptide association (Fig. 4E), when at the same time the orientational order at the level of the phospholipid head group is severely disturbed (Fig. 4A).

It is tempting to speculate that the resulting high peptide density within the membrane favors peptide-peptide interactions concomitant with β-sheet formation. The data do not reveal the oligomerisation state of GL13K in the membrane, however, it should be mentioned that the appearance of ^{15}N and ^{2}H spectra vary with solvents used during the sample preparation suggesting that the equilibria between mono- and oligomeric states are affected. In a related manner, increasing the pH in the absence of membranes results in the formation of β-sheet structures (Fig. 4C), whereas the randomized GL13-R1 sequence exhibits additional α-helical features (Fig. 4D). Such data are indicative that a propensity for β-sheet is inherent in the detailed amino acid arrangement of GL13K whereas the amino acid composition *per se* is in agreement with helical secondary structures.

In analogy with previous investigations [32, 47] the ensemble of data suggest that the GL13K-membrane interactions are governed by a number of equilibria encompassing random coil, α-helical, β-turn conformations as well as β-sheet aggregates (Fig 6). Catestatin has similarly been found to encompass a 7-residue α-helical conformation in micellar solutions with the remainder of the 21-residue peptide unstructured [48]. In contrast, the shortened cateslytin analogue exhibits CD spectra characteristic for β-turn sheet conformations in the presence of negatively charged liposomes [49]. Notably, the carboxy-terminal residue of cateslytin coincides with the helical boundary of catestatin suggesting that the missing residues stabilize the helical domain of catestatin. As a result of the missing intramolecular H-bonds typical for helical structures an intermolecular H-bonding network forms in the case of cateslytin. The cateslytin sequence and the GL13K peptides share a similar size (15 and 13 amino acid residues, respectively), a high density of positive charges (5+), as well as an α-helix – β-sheet transition/equilibrium in membrane environments (Fig. 6). The fusion peptide of HIV has also been found to exhibit an equilibrium between α-helical and β-turn secondary structures that is dependent on the lipid composition [50].

In its helical conformation the peptide probably interacts with the membrane interface through hydrophobic (3-4 leucines) and electrostatic interactions (4 lysines and the amino-terminus), which results in a wide range of topologies (Fig. 4B,C). At the same time the formation of aggregates is favored by high peptide densities at the membrane and the screening of excess positive charges on the peptide by anionic PG head groups. Thereby, the high surface concentration in the presence of POPG competes efficiently with helical membrane partitioning and results in the formation of β-sheets. In a related manner, the β-sheet secondary structures observed at high pH are probably a result of reduced repulsive electrostatic contributions (Fig. 3D).

Importantly, many cationic linear AMPs have been suggested to kill bacteria by forming openings in the cytoplasmic membranes that lead to the collapse of the electrochemical gradient and the release of intracellular contents. They do so by inserting their amphipathic structures into the membrane surface rather than by fully spanning the lipid bilayers [45, 51]. Potential mechanisms that have been proposed to explain the molecular structure of such membrane openings include, first, the formation of barrel stave arrangement (cf. [32, 47]).

Second, the 15-residue cationic peptide cateslytin has been suggested to form β-sheets oriented along the membrane surface. At peptide-to-lipid ratios of 1/15 these were shown to selectively interact with anionic lipids, to cause an increased order of the fatty acyl chains of negatively charged lipids and lateral phase separation of DMPC/DMPS 1/1 membranes [49]. The packing defects along the resulting phase boundaries are thought to be susceptible for membrane passage. Notably, here we found a strong membrane disordering effect, which is stronger on the zwitterionic PE than on the PG component of the mixed membranes (Figure 5).

Third, the partitioning of amphipathic peptides into the membrane interface has previously been shown to cause considerable curvature strain and to disrupt the membrane packing [45]. In the case of GL13K this effect is quite pronounced both when the global order of the oriented membranes is monitored by ^{31}P solid-state NMR spectroscopy (Fig. 3A) and when the fatty acyl chain order is investigated (Fig 5). It is thought that this can be due to molecules that partition in the membrane interface which thereby increase membrane curvature strain (Fig. 6). Interestingly the membrane disordering effect is more pronounced for POPE than the POPG in mixed membranes which is surprising considering that other cationic peptides have been shown to preferentially associate with the negatively charged lipid in PC/PS/cholesterol membranes [52].

Our results do not directly address the activity of GL13K in the more complex environment of bacterial biofilms that are organized in an extracellular matrix. However, the peptide-peptide interactions concomitant with β-sheet formation and the resulting membrane disruption may also affect bacterial interactions and disrupt their organization in biofilms. Indeed, when biofilms of *P. aeruginosa* are treated with GL13K the bacteria are killed and the biofilm appears to be destabilized and is dispersed or shed from the surface, as evidenced by scanning electron microscopy [7] .

Selectivity for bacterial versus healthy eukaryotic cells arises from the high negative surface charge and the high transmembrane electrical potential which lead to an increased concentration of the peptides along the prokaryotic surface [53, 54]. Therefore, the α-helical structure at the low peptide-to-lipid ratios that occur in the presence of zwitterionic membranes versus the β-sheet conformations observed when exposed to anionic lipids also reflect the selectivity of GL13K for bacterial cells and its lack of toxicity against eukaryotic cells. Furthermore, cholesterol protects the membranes of eukaryotic organisms. In general, the mode of interaction depends on peptide structure (distribution of hydrophilic and hydrophobic amino acids), peptide concentration and the physicochemical properties of the membrane [concept reviewed in [45]] suggesting that a delicate balance of interactions needs to be considered.

In conclusion, whereas the highly charged GL13K peptide exhibits strong attraction to negatively charged membranes hydrophobic association is rather weak. At low peptide-to detergent/lipid ratios the peptide adopts a helical conformation when interacting with membranes which converts to β-sheet-rich supramolecular arrangements with highly membrane disruptive properties. The high charge and small hydrophobic phase of this short peptide antibiotic thereby result in high conformational plasticity.

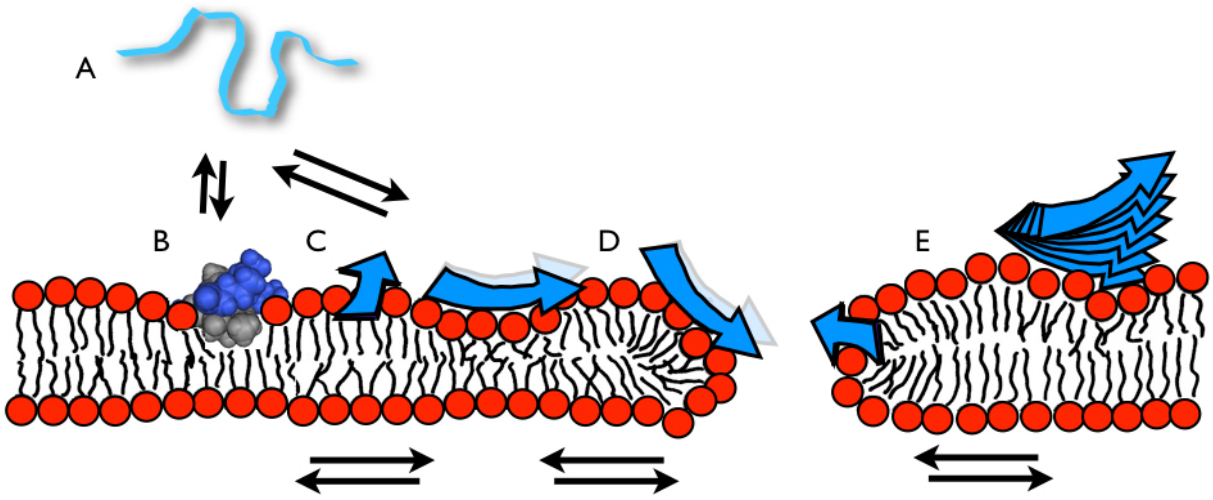

Figure 6: Model of the equilibria governing the random coil (A), helical-monomeric (B), β-strands (C, D) and β-sheet aggregates of GL13K (E). A membrane opening and a side-on aligned beta-sheet with its N-H vectors oriented parallel to the sample normal are shown in D. Notably, all of B-E can result in membrane deformations and ultimately bilayer openings.

Supporting information provides NMR resonance assignments and statistics on the structure calculations. More (CD spectra)

ACKNOWLEDGEMENTS

We are grateful to Delphine Hatey for the preparation of peptides. This research was supported by U.S. Public Health Service grants 1R01DE017989 from the National Institute for Dental and Craniofacial Research (SUG), GM 64742 from the National Institute for General Medical Sciences (GV) and a fellowship supported by R90DE023058 from the National Institute of Dental and Craniofacial Research (XC). Research funds from the University of Minnesota School of Dentistry (SUG) and The Office of the Vice-president for Research at the University of Minnesota, Project #55466 of the Grant-in-Aid of Research, Artistry and Scholarship Program (CA). BB was supported by a sabbatical stay at the University of Minnesota School of Dentistry that was generously supported by the School's Lasby Visiting Professor Fellowship and the University of Strasbourg. BB received additional support from the Agence Nationale de la Recherche (projects TRANSPEP 07-PCV-0018, membraneDNP 12-BSV5-0012, MemPepSyn 14-CE34-0001-01 and the LabEx Chemistry of Complex Systems 10-LABX-0026_CSC), the RTRA International Center of Frontier Research in Chemistry, the French Foundation for Medical Research (FRM), the University of Strasbourg, the CNRS, the Région Alsace.

References

[1] Fan, L., Sun, J., Zhou, M., Zhou, J., Lao, X., Zheng, H., and Xu, H. (2016) DRAMP: a comprehensive data repository of antimicrobial peptides, *Sci Rep 6*, 24482.

[2] Bechinger, B., and Gorr, S. U. (2017) Antimicrobial Peptides: Mechanisms of Action and Resistance, *Journal of dental research 96*, 254-260.

[3] Mikut, R., Ruden, S., Reischl, M., Breitling, F., Volkmer, R., and Hilpert, K. (2016) Improving short antimicrobial peptides despite elusive rules for activity, *Biochimica et Biophysica Acta (BBA) - Biomembranes 1858*, 1024-1033.

[4] Beamer, L. (2003) Structure of human BPI (bactericidal/permeability-increasing protein) and implications for related proteins., *Biochem. Soc. Trans. 31*, 791-794.

[5] Dankesreiter, S., Hoess, A., Schneider-Mergener, J., Wagner, H., and Miethke, T. (2000) Synthetic endotoxin-binding peptides block endotoxin-triggered TNF-{alpha} production by macrophages in vitro and in vivo and prevent endotoxin-mediated toxic shock, *Journal of Immunology 164*, 4804-4811.

[6] Abdolhosseini, M., Nandula, S. R., Song, J., Hirt, H., and Gorr, S. U. (2012) Lysine substitutions convert a bacterial-agglutinating peptide into a bactericidal peptide that retains anti-lipopolysaccharide activity and low hemolytic activity, *Peptides 35*, 231-238.

[7] Hirt, H., and Gorr, S. U. (2013) Antimicrobial peptide GL13K is effective in reducing biofilms of Pseudomonas aeruginosa, *Antimicrob Agents Chemother 57*, 4903-4910.

[8] Balhara, V., Schmidt, R., Gorr, S. U., and Dewolf, C. (2013) Membrane selectivity and biophysical studies of the antimicrobial peptide GL13K, *Biochimica et Biophysica Acta 1828*, 2193-2203.

[9] Verly, R. M., de Moraes, C. M., Resende, J. M., Aisenbrey, C., Bemquemer, M. P., Pilo-Veloso, D., Valente, A. P., Alemida, F. C., and Bechinger, B. (2009) Structure and membrane interactions of the antibiotic peptide dermadistinctin k by solution and oriented 15 N and 31 P solid-state NMR spectroscopy, *Biophys.J. 96*, 2194-2203.

[10] Bax, A. D., and Davis, D. G. (1985) MLEV-17-based two-dimensional homonuclear magnetization transfer spectroscopy, *Journal of Magnetic Resonance (1969) 65*, 355-360.

[11] Kumar, A., Ernst, R. R., and Wüthrich, K. (1980) A two-dimensional nuclear Overhauser enhancement (2D NOE) experiment for the elucidation of complete proton-proton cross-relaxation networks in biological macromolecules, *Biochemical and biophysical research communications 95*, 1-6.

[12] Piotto, M., Saudek, V., and SklenáŘ, V. (1992) Gradient-tailored excitation for single-quantum NMR spectroscopy of aqueous solutions, *Journal of biomolecular NMR 2*, 661-665.

[13] Shaka, A. J., Lee, C. J., and Pines, A. (1988) Iterative schemes for bilinear operators; application to spin decoupling, *Journal of Magnetic Resonance (1969) 77*, 274-293.

[14] Delaglio, F., Grzesiek, S., Vuister, G. W., Zhu, G., Pfeifer, J., and Bax, A. D. (1995) NMRPipe: a multidimensional spectral processing system based on UNIX pipes, *Journal of biomolecular NMR 6*, 277-293.

[15] Goddard, T. D., and Kneller, D. G. (2004) SPARKY 3, *University of California, San Francisco 14*, 15.

[16] Wuthrich, K. (1986) *NMR of proteins and nucleic acids*, Wiley.

[17] Schwieters, C. D., Kuszewski, J. J., Tjandra, N., and Marius Clore, G. (2003) The Xplor-NIH NMR molecular structure determination package, *Journal of Magnetic Resonance 160*, 65-73.

[18] Sreerama, N., and Woody, R. W. (2004) On the analysis of membrane protein circular dichroism spectra, *Protein Sci 13*, 100-112.
[19] Rance, M., and Byrd, R. A. (1983) Obtaining High-Fidelity Spin-1/2 Powder Spectra in Anisotropic Media: Phase-Cycled Hahn Echo Spectroscopy, *Journal of Magnetic Resonance 52*, 221-240.
[20] Davis, J. H., Jeffrey, K. R., Bloom, M., Valic, M. I., and Higgs, T. P. (1976) Quadrupolar Echo Deuteron Magnetic Resonance Spectroscopy in Ordered Hydrocarbon Chains, *Chem.Phys.Lett. 42*, 390-394.
[21] Seelig, J. (1977) Deuterium magnetic resonance: theory and application to lipid membranes, *Q.Rev.Biophys 10*, 353-418.
[22] Davis, J. H. (1983) The description of membrane lipid conformation, order and dynamics by 2 H-NMR, *Biochimica et Biophysica Acta 737*, 117-171.
[23] Salnikov, E., Bertani, P., Raap, J., and Bechinger, B. (2009) Analysis of the amide (15)N chemical shift tensor of the C(alpha) tetrasubstituted constituent of membrane-active peptaibols, the alpha-aminoisobutyric acid residue, compared to those of di- and tri-substituted proteinogenic amino acid residues, *J Biomol NMR 45*, 373-387.
[24] Olivieri, C., Buonocore, F., Picchietti, S., Taddei, A. R., Bernini, C., Scapigliati, G., Dicke, A. A., Vostrikov, V. V., Veglia, G., and Porcelli, F. (2015) Structure and membrane interactions of chionodracine, a piscidin-like antimicrobial peptide from the icefish Chionodraco hamatus, *Biochim Biophys Acta 1848*, 1285-1293.
[25] Porcelli, F., Verardi, R., Shi, L., Henzler-Wildman, K. A., Ramamoorthy, A., and Veglia, G. (2008) NMR structure of the cathelicidin-derived human antimicrobial peptide LL-37 in dodecylphosphocholine micelles, *Biochemistry-Us 47*, 5565-5572.
[26] Wishart, D. S., Sykes, B. D., and Richards, F. M. (1992) The chemical shift index: a fast and simple method for the assignment of protein secondary structure through NMR spectroscopy, *Biochemistry 31*, 1647-1651.
[27] Bechinger, B., Resende, J. M., and Aisenbrey, C. (2011) The structural and topological analysis of membrane-associated polypeptides by oriented solid-state NMR spectroscopy: Established concepts and novel developments, *Biophys Chem 153*, 115-125.
[28] Bechinger, B., and Salnikov, E. S. (2012) The membrane interactions of antimicrobial peptides revealed by solid-state NMR spectroscopy, *Chem Phys Lipids 165*, 282-301.
[29] Kim, C., Spano, J., Park, E. K., and Wi, S. (2009) Evidence of pores and thinned lipid bilayers induced in oriented lipid membranes interacting with the antimicrobial peptides, magainin-2 and aurein-3.3, *Biochim. Biophys. Acta 1788*, 1482-1496.
[30] Hallock, K. J., Lee, D. K., Omnaas, J., Mosberg, H. I., and Ramamoorthy, A. (2002) Membrane composition determines pardaxin's mechanism of lipid bilayer disruption, *Biophys J 83*, 1004-1013.
[31] Resende, J. M., Verly, R. M., Aisenbrey, C., Amary, C., Bertani, P., Pilo-Veloso, D., and Bechinger, B. (2014) Membrane interactions of Phylloseptin-1, -2, and -3 peptides by oriented solid-state NMR spectroscopy, *Biophys. J. 107*, 901-911
[32] Salnikov, E., Aisenbrey, C., Balandin, S. V., Zhmak, M. N., Ovchinnikova, A. Y., and Bechinger, B. (2011) Structure and alignment of the membrane-associated antimicrobial peptide arenicin by oriented solid-state NMR spectroscopy, *Biochemistry-Us 50*, 3784-3795.
[33] Yamaguchi, S., Hong, T., Waring, A., Lehrer, R. I., and Hong, M. (2002) Solid-state NMR investigations of peptide-lipid interaction and orientation of a beta-sheet antimicrobial peptide, protegrin, *Biochemistry-Us 41*, 9852-9862.

[34] Bechinger, B., and Sizun, C. (2003) Alignment and structural analysis of membrane polypeptides by 15N and 31P solid-state NMR spectroscopy *Concepts in Magnetic Resonance 18A*, 130 -145
[35] Aisenbrey, C., and Bechinger, B. (2004) Tilt and rotational pitch angles of membrane-inserted polypeptides from combined 15N and 2H solid-state NMR spectroscopy *Biochemistry-Us 43*, 10502-10512.
[36] Sanders, C. R., 2nd, and Landis, G. C. (1995) Reconstitution of membrane proteins into lipid-rich bilayered mixed micelles for NMR studies, *Biochemistry-Us 34*, 4030-4040.
[37] Sanders, C. R., and Prosser, R. S. (1998) Bicelles - A model membrane system for all seasons, *Structure 6*, 1227-1234.
[38] Seelig, J. (1978) 31P nuclear magnetic resonance and the head group structure of phospholipids in membranes, *Biochim Biophys Acta 515*, 105-140.
[39] Yeagle, P. L. (1990) Phosphorus NMR of Membranes, In *Biological Magnetic Resonance*, pp 1-54, Plenum Press, New York.
[40] Prosser, R. S., Hwang, J. S., and Vold, R. R. (1998) Magnetically aligned phospholipid bilayers with positive ordering: a new model membrane system, *Biophys J 74*, 2405-2418.
[41] Tan, A., Ziegler, A., Steinbauer, B., and Seelig, J. (2002) Thermodynamics of sodium dodecyl sulfate partitioning into lipid membranes, *Biophys J 83*, 1547-1556.
[42] Aisenbrey, C., and Bechinger, B. (2004) Investigations of peptide rotational diffusion in aligned membranes by 2H and 15N solid-state NMR spectroscopy *J.Am.Chem.Soc. 126*, 16676-16683.
[43] Salnikov, E. S., Mason, A. J., and Bechinger, B. (2009) Membrane order perturbation in the presence of antimicrobial peptides by 2 H solid-state NMR spectroscopy, *Biochimie 91*, 743.
[44] Wieprecht, T., Beyermann, M., and Seelig, J. (1999) Binding of antibacterial magainin peptides to electrically neutral membranes: Thermodynamics and structure, *Biochemistry-Us 38*, 10377-10378.
[45] Bechinger, B. (2015) The SMART model: Soft Membranes Adapt and Respond, also Transiently, to external stimuli, *J. Peptide Sci. 21*, 346-355
[46] Lauterwein, J., Bosch, C., Brown, L. R., and WÅthrich, K. (1979) Physicochemical studies of the protein-lipid interactions in melittin-containing micelles, *Biochimica et Biophysica Acta 556*, 244-264.
[47] Mani, R., Cady, S. D., Tang, M., Waring, A. J., Lehrer, R. I., and Hong, M. (2006) Membrane-dependent oligomeric structure and pore formation of a beta-hairpin antimicrobial peptide in lipid bilayers from solid-state NMR, *Proc.Natl.Acad.Sci.U.S.A 103*, 16242-16247.
[48] Sugewara, M., Resende, J. M., Moraes, C. M., Metz-Boutigue, M. H., and Bechinger, B. (2010) Structure and interactions in membranes of human and bovine Catestatin by solution and solid-state NMR spectroscopy, *Faseb J 24*, 1737-1746
[49] Jean-Francois, F., Castano, S., Desbat, B., Odaert, B., Roux, M., Metz-Boutigue, M. H., and Dufourc, E. J. (2008) Aggregation of cateslytin beta-sheets on negatively charged lipids promotes rigid membrane domains. A new mode of action for antimicrobial peptides?, *Biochemistry-Us 47*, 6394-6402.
[50] Lai, A. L., Moorthy, A. E., Li, Y., and Tamm, L. K. (2012) Fusion activity of HIV gp41 fusion domain is related to its secondary structure and depth of membrane insertion in a cholesterol-dependent fashion, *J Mol Biol 418*, 3-15.
[51] Shai, Y. (2002) Mode of action of membrane active antimicrobial peptides, *Biopolymers 66*, 236-248.

[52] Mason, A. J., Martinez, A., Glaubitz, C., Danos, O., Kichler, A., and Bechinger, B. (2006) The antibiotic and DNA-transfecting peptide LAH4 selectively associates with, and disorders, anionic lipids in mixed membranes, *FASEB J. 20*, 320-322.
[53] Matsuzaki, K., Nakamura, A., Murase, O., Sugishita, K., Fujii, N., and Miyajima, K. (1997) Modulation of magainin 2-lipid bilayer interactions by peptide charge, *Biochemistry-Us 36*, 2104-2111.
[54] Wenk, M., and Seelig, J. (1998) Magainin 2 amide interaction with lipid membranes: Calorimetric detection of peptide binding and pore formation, *Biochemistry-Us 37*, 3909-3916.

TOC graphics (for Table of Contents use only)